A battery-operated atmospheric-pressure plasma wand for biomedical applications

2014 J. Phys. D: Appl. Phys. 47 145204

(http://iopscience.iop.org/0022-3727/47/14/145204)

IOP Publishing Journal of Physics D: Applied Physics
J. Phys. D: Appl. Phys. **47** (2014) 145204 (6pp) doi:10.1088/0022-3727/47/14/145204

A battery-operated atmospheric-pressure plasma wand for biomedical applications

X Pei, J Liu, Y Xian and X Lu[1]

State Key Laboratory of Advanced Electromagnetic Engineering and Technology, Huazhong University of Science and Technology, Wuhan, Hubei 430074, People's Republic of China

E-mail: luxinpei@hotmail.com

Received 10 January 2014, revised 11 February 2014
Accepted for publication 17 February 2014
Published 21 March 2014

Abstract

A handheld, battery-operated atmospheric-pressure plasma rod (named the plasma wand) which does not rely on an external power source (e.g. mains power or a power generator) or gas supply is reported. The plasma wand can be used for killing bacteria, fungi or viruses that are hidden in narrow channels such as the nasal cavity and ear canal, which are difficult to access using most currently available devices. Besides, the electrical characterization, plasma wand temperature, emission spectra of the plasma, ozone and OH radical concentration generated by the device, are investigated by different diagnostic methods. The ozone concentration reaches 120 ppm 1 mm away from the device and the OH concentration reaches 3.5×10^{14} cm^{-3} in the plasma. The preliminary bacteria inactivation experiment results show that all the bacteria samples on the microfiltration membrane are killed by this device within 30 s.

Keywords: atmospheric-pressure plasma, biomedical application, plasma jet

(Some figures may appear in colour only in the online journal)

1. Introduction

In the past decade room-temperature atmospheric-pressure plasma jets (RT-APPJs) have attracted a lot of attention due to their applications in the field of health care and medicine, including bacteria inactivation, blood coagulation, wound healing, teeth whitening, and tooth root canal treatment [1–9]. To fulfil the specific requirements of various applications, many different types of RT-APPJs with different designs and driven by different power sources, including kHz ac, RF, microwave, pulsed dc and dc voltages, have been developed. However, external power sources (e.g. mains power or a power generator) are needed for all these devices [10–16]. In addition, most of these devices also need a gas supply (e.g. He, Ar). Furthermore, for applications where bacteria, fungi, or viruses are hidden in narrow channels such as the nasal cavity and ear canal, most currently available devices are not suitable [17–23].

In this paper, a battery-operated handheld plasma source, named the plasma wand, is reported. This device is driven by a battery without an external power source. It can generate plasmas in the surrounding air without an extra noble gas supply. There is no feeling of heat or electrical shock at all when one holds the plasma wand. The characteristics of the device, including the electrical characterization, temperature of the plasma wand, emission spectra of the plasma, ozone and OH radical concentration generated by the plasma, are investigated. A bacterial inactivation experiment shows that the device can effectively kill bacteria.

2. Experiment setup

Figure 1(*a*) is schematic of the experimental setup. The device consists of two HV electrodes (an outside electrode and inside electrode) and a dielectric tube. A one-ended closed stainless steel mesh tube is used as the ground outside electrode. The inner diameter and thickness of the stainless steel mesh tube are 5 mm and 0.1 mm, respectively. The diameter of the meshes is 0.8 mm. The inside electrode, which is made of a copper wire with a diameter of 4 mm, is connected to a pulsed ac booster output. The pulse ac booster is driven by a 12 V lithium battery. The frequency of the ac booster is fixed at about 25 kHz. The duty cycle of the ac booster can be adjusted from 5% to 100%. A ceramic tube with one end closed is placed between the

[1] Author to whom any correspondence should be addressed.

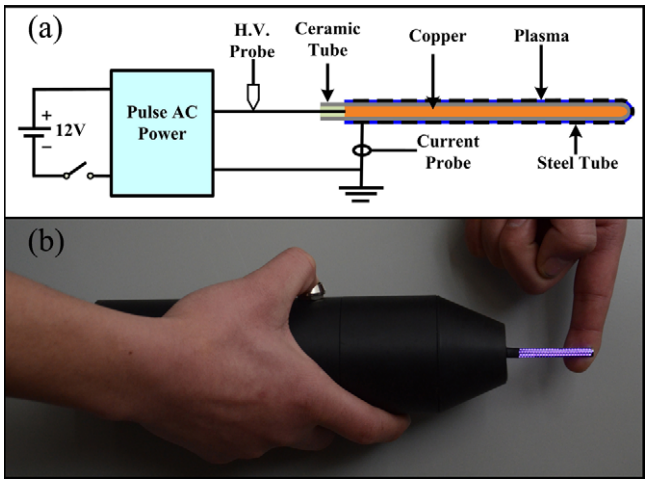

Figure 1. (*a*) Schematic of the experimental setup. (*b*) Photograph of the handheld atmospheric-pressure plasma wand device.

two electrodes. The inner diameter of the ceramic tube is the same as the diameter of the inner copper electrode while the outer diameter of the ceramic tube is the same as the inner diameter of the stainless steel mesh tube. The lengths of the mesh electrode and the ceramic tube are 50 mm and 60 mm, respectively. When a 12 V voltage is applied to pulse the ac booster, a bright plasma rod, named here 'the plasma wand', is generated as shown in figure 1(*b*). It can be hold by a human being without any feeling of heat or electrical shock.

3. Experiment results

To study the I–V characteristics of the plasma, a P6015 Tektronix HV probe is used to measure the voltage on the HV electrode, and a Pearson current monitor (model 2877) is used to measure the discharge current. The voltage and current waveforms are recorded by a Tektronix DPO7104 wide band digital oscilloscope. Figure 2(*a*) shows the I–V characteristics of the discharge when the duty cycle of the power supply is 10%. Figure 2(*b*) is the close-up of the current and voltage waveforms of about two cycles. As can be seen from this figure, the peak-to-peak voltage is about 9 kV and the discharge current appears with many filament peaks per cycle of the applied voltage. The maximum current pulse has a peak of about 30 mA. It is a typical surface dielectric-barrier discharge (DBD) discharge.

In order to estimate the power consumption by the plasma rod, the Lissajous-figure method is used by connecting a large capacitor (5 nF) in series in the discharge circuit. The average power consumed by the plasma rod can be determined from a Lissajous figure as shown in figure 3. This typical Lissajous ellipsoid relates the charge Q to the applied voltage during a single period of the applied voltage. By calculating the area of the Lissajous figure in figure 3, the average power consumption of the plasma rod is about 12 W when the duty cycle of the pulse ac booster is 10%.

The temperature on the stainless steel tube of the plasma wand was measured by an infrared thermometer when the discharge condition is the same as that in figure 2. Figure 4

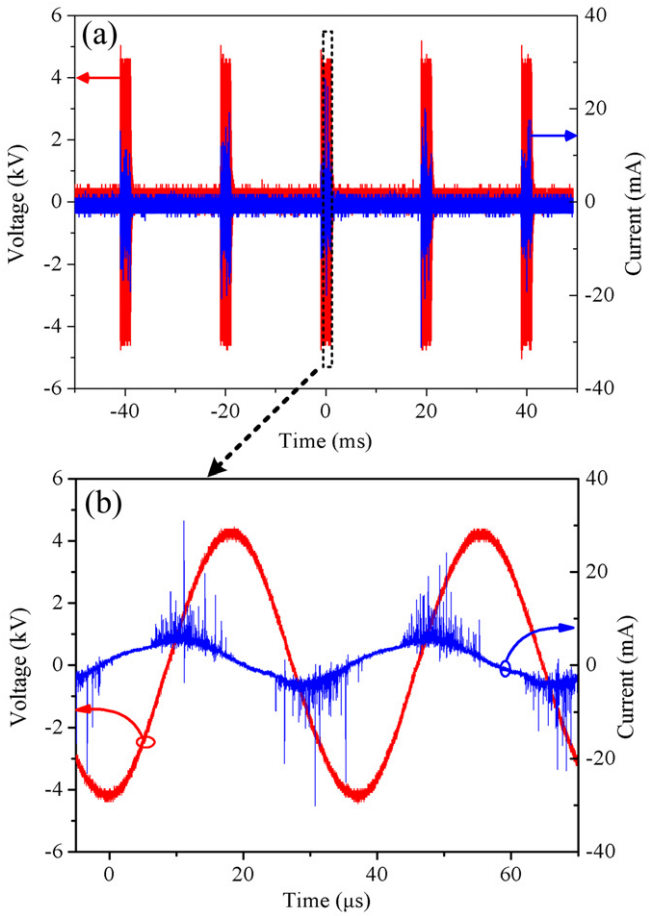

Figure 2. (*a*) I–V characteristics of the discharge when the duty cycle of the power supply is 10%. (*b*) The current and voltage waveforms at a higher magnification.

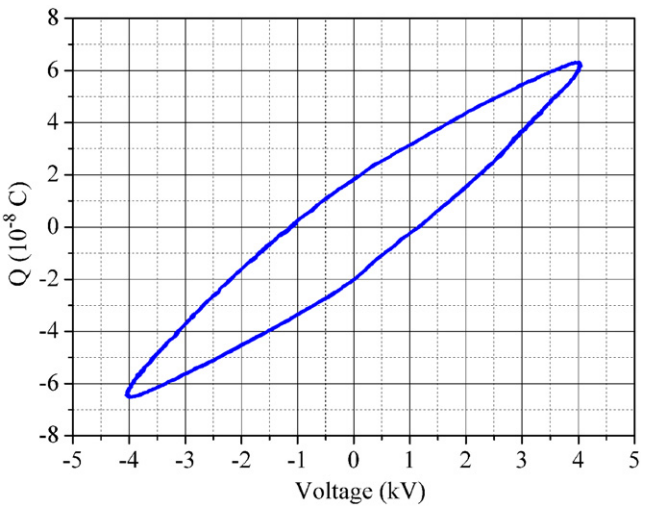

Figure 3. Lissajous figure for the discharge driven by the pulsed ac booster supply. The discharge operation parameters are the same as in figure 2.

shows the time dependent temperature behaviour. It can be seen clearly that the temperature of the plasma rod reaches its maximum of about 38 °C after operating for about 5 min. Then it stays at about 38 °C. The maximum temperature of the

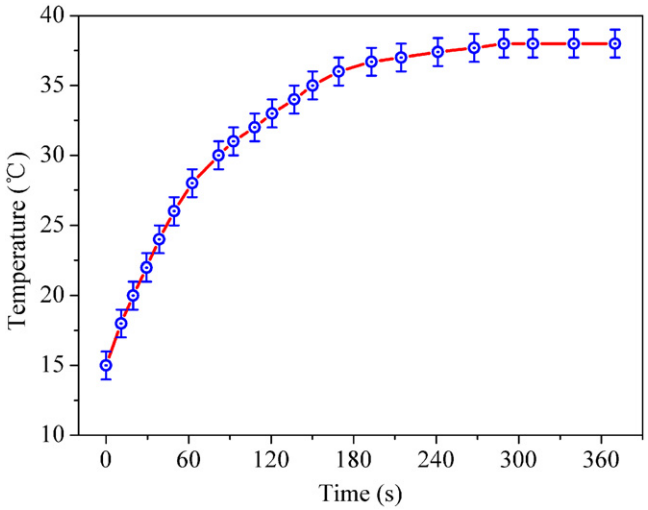

Figure 4. Temperature variation with the discharge time on the stainless steel tube of the plasma wand device.

plasma wand allows numerous applications in plasma health care and medicine.

To know what kind of reactive species are present in the plasma, a half-metre spectrometer (Princeton Instruments Acton SpectraHub 2500i; grating: 1200 g mm^{-1}, slit width: 80 μm) is used to measure the optical emission spectrum (OES) of the plasma. Figures 5(*a*) and (*b*) display the emission spectra of the plasma from 250 nm to 500 nm and 500 nm to 850 nm, respectively. It shows clearly that the spectrum is dominated by N_2 emission. Moreover, there is also an O-atom emission. As we know, O atoms are very active and play a very important role in the applications of plasma medicine [24]. From the simulations of reactive oxygen plasma species (especially O atoms) interacting with bacterial cell walls [25–27], they found the chemical reactivity of these reactive oxygen species warranted the effectiveness of plasmas for decontamination and sterilization purposes.

In order to learn more about the reactive species generated by the plasma, the ozone density at different positions around the plasma rod is measured by UV absorption spectroscopy. Ozone which has long lifetime (an hour or longer) [28] is a well-known reactive agent for the proliferation of cells, disinfection of wounds and blood ozonation [29]. Figure 6(*a*) shows the experimental setup for the measurement of ozone concentration around the plasma rod. A calibration light source (Ocean Optics, DH-2000-CAL) which can emit the 254 nm UV line is used. The UV light goes through a convex quartz lens (f = 500 mm) and focuses at the location of the plasma rod, then the light is collected by another convex quartz lens (f = 500 mm) and is projected on the entrance slit of a half-metre spectrometer (grating: 1200 g mm^{-1}, slit width: 80 μm). The intensity of the UV light is measured by the spectrometer. The distance d between the light beam and the plasma rod is adjustable. The density of ozone can be estimated by the equation below [30]

$$O_3(\text{ppm}) = \frac{10^6 T}{273 P k l} \log \frac{I_0}{I_t}, \qquad (1)$$

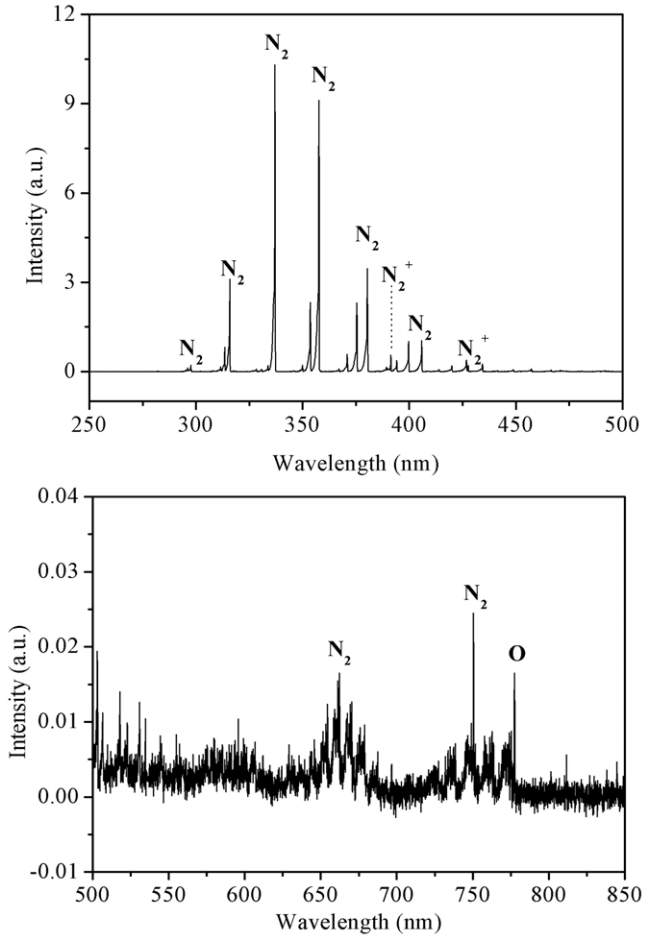

Figure 5. Optical emission spectrum in the range from 250 to 850 nm of the plasmas in the open air. The discharge operation parameters are the same as in figure 2.

where T is the temperature, K; P is the total pressure, atm; k is the extinction coefficient, 134 cm^{-1} atm^{-1} at STP for ozone; l is the absorption length, ~5 cm; I_0 is the intensity of the incident UV light with carrier gas only; and I_t is the intensity of the transmitted UV light with O_3 present.

According to the relative emission intensity of the 254 nm line measured by the spectrometer, the I_0/I_t ratio can be obtained. The gas temperature around the plasma rod (not on the steel tube) can be treated as a constant. Thus the O_3 concentration can be easy obtained according to equation (1).

Figure 6(*b*) shows the obtained ozone concentration for different d. It is about 120 ppm for d of 1 mm and it decreases quickly with the increase of d. It should be pointed out that the plasma generated by this device mostly appears near the meshes of the stainless steel tube. There is no plasma in the detected region for d of 1 mm. However, the ozone concentration is still quite high even at the distance of 5 mm away from the plasma rod.

OH is another important reactive agent that is generated by cold atmospheric-pressure plasmas. OH species can enhance chemical reactions and also have a destructive effect on the fatty acid side-chains of lipids in various membranes such as mitochondrial membranes of cells [31]. The interaction of OH with lipids also had been modelled and demonstrated by

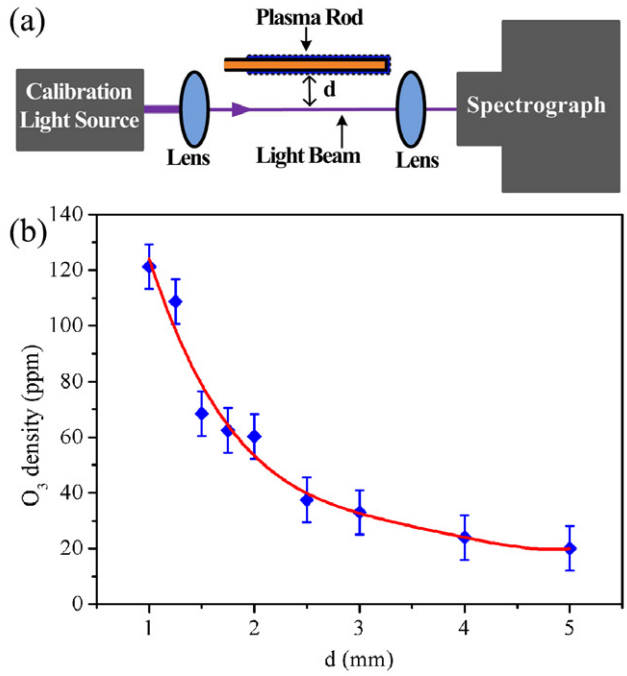

Figure 6. (*a*) Experimental setup for measurement of ozone around the plasma rod, (*b*) absolute concentration of ozone for different d. d is the distance between the laser beam and the plasma rod. The discharge operation parameters are the same as in figure 2.

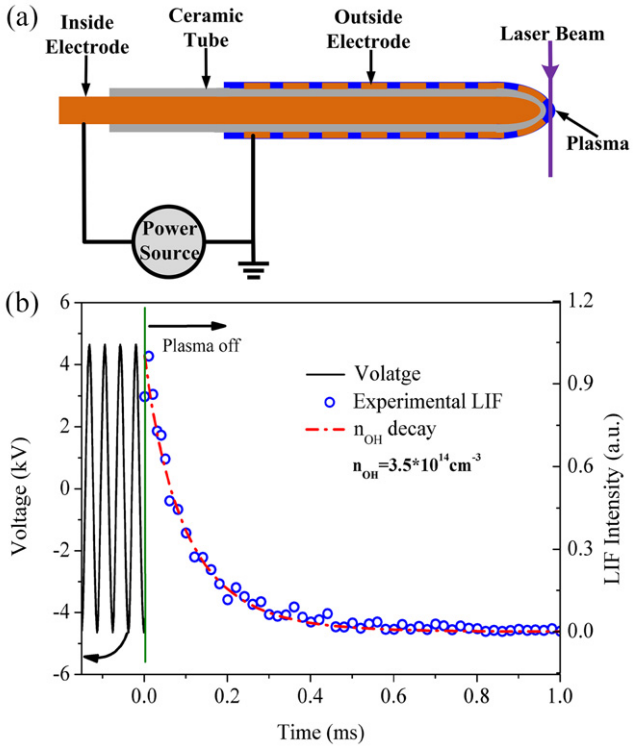

Figure 7. (*a*) LIF experiment setup for the measurement of OH radicals in the plasma. (*b*) Characteristic decay curve of OH LIF signal under the same experimental conditions as in figure 2. The blue ring symbol is the experimental LIF signal. The red dash–dot line is the simulation result using the OH radical decay model. Model parameters are: $n_{OH} = 3.5 \times 10^{14}\,\mathrm{cm}^{-3}$, $k_1 = 10.4 \times 10^{-12}\,\mathrm{cm}^3\,\mathrm{s}^{-1}$, $k_2 = 3900\,\mathrm{s}^{-1}$, $b = 200\,\mathrm{s}^{-1}$, $C = 3500\,\mathrm{s}^{-1}$.

Van der Paal *et al* [32]. Their calculations predicted that the OH radicals can increase the hydrophilic character of the fatty acids and change the general lipid composition of the skin. Thus, the OH radical concentration is also measured in our experiments. Here a laser-induced fluorescence (LIF) is used to measure the OH radical density inside the plasma. The absolute OH density is estimated by the decay model which considered the most important loss processes of OH radical after the discharge. This method has been successfully used in many LIF measurements for plasma sources in different atmospheres [33–37].

A dye laser (Radiant Dyes, NarrowScan) pumped by a YAG : Nd laser (Continuum, SURELTTE III-10) which was also used in our previous study [38] at 532 nm is used for exciting OH radicals with 80 μJ energy per pulse. The dye laser wavelength (~282.6 nm) is set to excite the $P_1(2)$ branch of the OH [$(A\,^2\sum, \upsilon' = 1)$–$(X\,^2\prod, \upsilon'' = 0)$] band. The diameter of the beam at the position of the plasma is about 0.5 mm. The laser beam passes through the plasma near the tip of the outer electrode where it can achieve a good fluorescence signal as shown in figure 7(*a*). Perpendicular to the laser beam, the fluorescence light is captured by an ICCD camera ((PIMAX2; exposure time: 100 ns) through a 309 nm narrow-band filter.

Figure 7(*b*) shows the time evolution of OH LIF intensity after the plasma is switched off. The discharge parameters are the same as in figure 2.The blue ring symbol is the experimental LIF signal which decays with time. The red dash–dot line is the simulation result using the OH radical decay model, which was previously used for atmospheric DBD plasmas [37]. In this model, most of the OH loss mechanisms are considered including 'self-destruction' processes and reactions with other species including NO, NO_2 O, H, O_2, O_3, H_2O_2, etc. [38]. The OH decay behaviour can be described by the following equation:

$$\frac{\mathrm{d[OH]}}{\mathrm{d}t} = -k_1[\mathrm{OH}]^2 - (k_2\mathrm{e}^{-bt} + C)[\mathrm{OH}], \qquad (2)$$

where $-k_1[\mathrm{OH}]^2$ is the quadratic self-destruction term. $-(k_2\mathrm{e}^{-bt} + C)[\mathrm{OH}]$ is the term of reactions with other species and diffusion. When the simulation result fits very well with the experimental LIF signal as shown in figure 7(*b*), the initial OH absolute density (at 1 μs) can be estimated as $3.5 \times 10^{14}\,\mathrm{cm}^{-3}$ in the plasma. Here the fitting parameters are chosen as $k_1 = 10.4 \times 10^{-12}\,\mathrm{cm}^3\,\mathrm{s}^{-1}$, $k_2 = 3900\,\mathrm{s}^{-1}$, $b = 200\,\mathrm{s}^{-1}$ and $C = 3500\,\mathrm{s}^{-1}$. It is worth noting that this absolute OH density is inside the plasma produced by the surface DBD. Unlike the ozone concentration distribution presented above, there is no obvious OH LIF signal outside the plasma.

Finally, a preliminary bacteria inactivation experiment has been carried out. The Bacillus coli bacteria are used in this experiment. The bacterial samples treated by this device were prepared as follows. First, a bacterial culture with the concentration of about 10^8 CFU ml^{-1} (CFU: colony-forming unit) is prepared and then the culture is diluted to 10^6 CFU ml^{-1} for this experiment. Then, 0.2 ml of this diluted

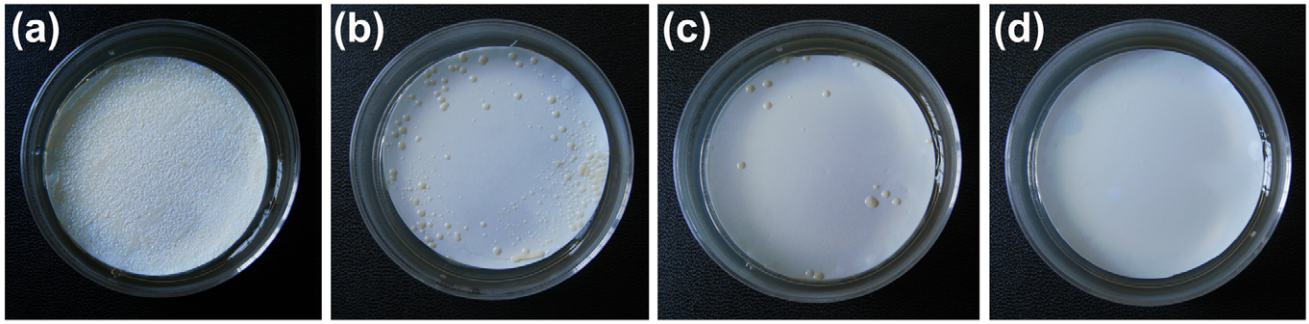

Figure 8. Photographs of *Bacillus coli* samples on the microfiltration membrane in Petri dishes treated by the plasma wand. The microfiltration membrane with bacterial samples is spread out on the agar plates in Petri dishes. (*a*) Control experiment. (*b*)–(*d*) The treatment time is 5 s, 15 s, and 30 s, respectively.

suspension is evenly spread over a microfiltration membrane which has same size as the Petri dish (diameter: 5 cm). The bacterial samples can take up nutrients through the microspores of the microfiltration membrane and grow on it. Next, this microfiltration membrane taken with bacterial samples is placed on the inner surface of a quartz tube with one end closed (inner diameter: 25 mm, length: 50 mm). Then the plasma rod is inserted into the centre of the quartz tube and it is then switched on to treat the bacterial samples for different lengths of time. After the plasma treatment, the microfiltration membrane with bacterial samples is taken out from the quartz tube immediately and then placed on the agar plates in Petri dishes. Next, the Petri plates are put into an oven and incubated for 24 h at 37 °C. For the control experiments, the bacterial samples on the microfiltration membrane are treated similarly but with the plasma switched off. It should be pointed out that all the experiments reported in this paper are repeated three times, and the results are consistent with the same experimental conditions.

Figures 8(*a*)–(*d*) shows the experiment results. The white areas suggest the effective killing of bacteria in these areas. On the other hand, the grey points suggest that bacteria grow there. As we can see from the control experiment result (figure 8(*a*)), the bacteria grow on the entire surface of the microfiltration membrane. When the plasma is on, as shown in figures 8(*b*)–(*d*), the growth of bacteria is affected significantly. We can see clearly that all the bacteria on the microfiltration membrane are inactivated when the treatment time is 30 s.

Compared with the recent inactivation results achieved by different atmospheric-pressure plasma sources (such as plasma jets, plasma needles, etc.), the plasma wand device has a very high sterilization efficiency. Kim *et al* [39] treated *E. coli* using an atmospheric pressure single pin electrode plasma jet (power consumption 8 W). It needed at least 60 s to inactivate all the bacteria. Shimizu *et al* [40] reported a microwave plasma torch (power consumption 85 W) to inactivate *E. coli* with a treatment time of 4 min. Of course, it is difficult to conclude which device is the best due to the different sensibility of living biological material and different surrounding conditions. More importantly, as pointed out in the beginning, this device is especially designed for the decontamination of narrow channels such as the nasal cavity and ear canal, where most current devices are not applicable.

4. Conclusion

In conclusion, a battery-operated handheld surface DBD plasma source which is designed for the treatment of narrow and deep channels such as the nasal cavity is reported. The temperature on the plasma wand stays at about 38 °C after operation for about 5 min and the outside electrode is grounded. So there is no feeling of heat or electrical shock at all when one holds the plasma wand. From the Lissajous figure of the discharge, the power consumption is estimated to be about 12 W when the duty cycle of the power supply is 10%. The ozone density is about 120 ppm at 1 mm from the plasma rod. Using the LIF technique, the OH radical density in the plasma is estimated to be about 3.5×10^{14} cm^{-3}. Preliminary bacterial inactivation experimental results show that the device has a very high sterilization efficiency.

Acknowledgments

This work was partially supported by the National Natural Science Foundation (grant no 51077063, 51277087), the Research Fund for the Doctoral Programme of Higher Education of China (20100142110005) and Chang Jiang Scholars Programme, Ministry of Education, People's Republic of China.

References

[1] Laroussi M, Richardson J and Dobbs F 2002 *Appl. Phys. Lett.* **81** 772
[2] Mariotti D 2008 *Appl. Phys. Lett.* **92** 151505
[3] Douat C, Bauville G, Fleury M, Laroussi M and Puech V 2012 *Plasma Sources Sci. Technol.* **21** 034010
[4] Fridman G, Peddinghaus M, Ayan H, Fridman A, Balasubramanian M, Gutsol A, Brooks A and Friedman G 2006 *Plasma Chem. Plasma Process.* **26** 425
[5] Reuter S, Niemi K, Gathern V and Dobele H 2009 *Plasma Sources Sci. Technol.* **18** 015006
[6] Lee H W, Kim G J, Kim J M, Park J K, Lee J K and Kim G C 2009 *J. Endodontics* **35** 587
[7] Nikiforov A, Sarani A and Leys C 2011 *Plasma Sources Sci. Technol.* **20** 015014
[8] Lu X, Jiang Z, Xiong Q, Tang Z, Hu X and Pan Y 2008 *Appl. Phys. Lett.* **92** 081502

[9] Ostrikov K, Neyts E C and Meyyappan M 2013 *Adv. Phys.* **62** 113
[10] Huang J, Li H, Chen W, Lv G, Wang X, Zhang G, Ostrikov K, Wang P and Yang S 2011 *Appl. Phys. Lett.* **99** 253701
[11] Kolb J, Mohamed A, Price R, Swanson R, Bowman A, Chiavarini R, Stacey M and Schoenbach K 2008 *Appl. Phys. Lett.* **92** 241501
[12] Wang D, Zhao D, Feng K, Zhang X, Liu D and Yang S 2011 *Appl. Phys. Lett.* **98** 161501
[13] Keidar M and Beilis I 2009 *Appl. Phys. Lett.* **94** 191501
[14] Shashurin A, Keidar M, Bronnikov S, Jurjus R A and Stepp M A 2008 *Appl. Phys. Lett.* **93** 181501
[15] Sands B, Ganguly B and Tachibana K 2008 *Appl. Phys. Lett.* **92** 151503
[16] Xiong Z, Robert E, Sarron V, Pouvesle J and Kushner M 2013 *J. Phys. D: Appl. Phys.* **46** 155203
[17] Shashurin A, Keidar M, Bronnikov S, Jurjus R and Stepp M 2008 *Appl. Phys. Lett.* **93** 181501
[18] Shashurin A, Keidar M, Bronnikov S, Jurjus R A and Stepp M A 2008 *Appl. Phys. Lett.* **93** 181501
[19] Pei X, Lu X, Liu J, Liu D, Yang Y, Ostrikov K, Chu P K and Pan Y 2012 *J. Phys. D: Appl. Phys.* **45** 165205
[20] Lu X, Laroussi M and Puech V 2012 *Plasma Sources Sci. Technol.* **21** 034005
[21] Laroussi M and Lu X 2005 *Appl. Phys. Lett.* **87** 113902
[22] Mariotti D, Svrcek V and Kim D G 2007 *Appl. Phys. Lett.* **91** 183111
[23] Xian Y, Zhang P, Lu X, Pei X, Wu S, Xiong Q and Ostrikov K 2013 *Sci. Rep.* **3** 1599
[24] Lu X, Ye T, Cao Y G, Sun Z Y, Xiong Q, Tang Z Y, Xiong Z L, Hu J, Jiang Z H and Pan Y 2008 *J. Appl. Phys.* **104** 053309
[25] Yusupov M, Bogaerts A, Huygh S, Snoeckx R, van Duin A C T and Neyts E C 2013 *J. Phys. Chem.* C **117** 5993
[26] Yusupov M, Neyts E C, Khalilov U, Snoeckx R, van Duin A C T and Bogaerts A 2012 *New J. Phys.* **14** 093043
[27] Babaeva N Y, Ning N, Graves D B, and Kushner M J 2012 *J. Phys. D: Appl. Phys.* **45** 115203
[28] Sakalys J and Girgzdiene R 2010 *Lith. J. Phys.* **50** 247
[29] Kuhn S, Bibinov N, Gesche R and Awakowicz P 2010 *Plasma Sources Sci. Technol.* **19** 015013
[30] Assembly of Life Sciences (US). Committee on Medical and Biologic Effects of Environmental Pollutants 1977 *Ozone and Other Photochemical Oxidants* (Washington DC: National Academy of Sciences)
[31] Pei X, Lu Y, Wu S, Xiong Q and Lu X 2013 *Plasma Sources Sci. Technol.* **22** 025023
[32] Van der Paal J, Aernouts S, van Duin A C T, Neyts E C and Bogaerts A 2013 *J. Phys. D: Appl. Phys.* 46 395201
[33] Ono R and Oda T 2002 *J. Phys. D: Appl. Phys.* **35** 2133
[34] Verreycken T, Horst R, Baede A, Veldhuizen E and Bruggeman P J 2012 *J. Phys. D: Appl. Phys.* **45** 045205
[35] Nakagawa Y, Ono R and Oda T 2011 *J. Appl. Phys.* **110** 073304
[36] Tochikubo F, Uchida S and Watanabe T 2004 *Japan. J. Appl. Phys.* **43** 315
[37] Dilecce G, Ambrico P F, Simek M and De Benedictis S 2012 *Chem. Phys.* **398** 142
[38] Sakiyama Y, Graves D B, Chang H W, Shimizu T and Morfill G E 2012 *J. Phys. D: Appl. Phys.* **45** 425201
[39] Kim S J, Chung T H, Bae S H and Leem S H 2009 *Appl. Phys. Lett.* **94** 141502
[40] Shimizu T *et al* 2008 *Plasma Process. Polym.* **5** 577